Hindawi Publishing Corporation
EURASIP Journal on Wireless Communications and Networking
Volume 2008, Article ID 173645, 11 pages
doi:10.1155/2008/173645

Research Article

On Intercell Interference and Its Cancellation in Cellular Multicarrier CDMA Systems

Simon Plass

German Aerospace Center (DLR), Institute of Communications and Navigation, Oberpfaffenhofen, 82234 Wessling, Germany

Correspondence should be addressed to Simon Plass, simon.plass@dlr.de

Received 2 May 2007; Accepted 17 September 2007

Recommended by Luc Vandendorpe

The handling of intercell interference at the cell border area is a strong demand in future communication systems to guarantee efficient use of the available bandwidth. Therefore, this paper focuses on the application of iterative intercell interference cancellation schemes in cellular multicarrier code division multiple access (MC-CDMA) systems at the receiver side for the downlink. First, the influence of the interfering base stations to the total intercell interference is investigated. Then, different concepts for intercell interference cancellation are described and investigated for scenarios with several interfering cells. The first approach is based on the use of the hard decision of the demodulator to reconstruct the received signals. This does not require the higher amount of complexity compared to the second approach which is based on the use of the more reliable soft values from the decoding process. Furthermore, the extrinsic information as a reliability measure of this soft iterative cancellation process is investigated in more detail based on the geographical position of the mobile terminal. Both approaches show significant performance gains in the severe cell border area. With the soft intercell interference cancellation scheme, it is possible to reach the single-user bound. Therefore, the intercell interference can be almost eliminated.

1. INTRODUCTION

The high data rate demands of next generation mobile communication systems require a very efficient exploitation of the available spectrum. Therefore, future cellular mobile concepts reuse the whole spectrum in each served cell [1] which corresponds to a frequency reuse of one. By applying the same frequency band in neighboring cells, the cell border areas are highly influenced by intercell interference. This causes severe performance degradations or even connection loss.

Technologies which are currently considered candidates for these future communication systems are based on the generalized multicarrier (GMC) concept [2, 3]. The technology multicarrier code division multiple access (MC-CDMA) [4, 5] is within the GMC concept and combines the benefits of multicarrier transmission and spread spectrum. Multicarrier transmission, namely, orthogonal frequency division multiplexing (OFDM) [6], offers simple digital realization due to the fast Fourier transformation (FFT) operation and low complex receivers. Additionally, spread spectrum, namely code division multiple access (CDMA), gives high flexibility, robustness, and frequency diversity gains [7]. Recently, the cellular aspects of MC-CDMA were investigated. In [8, 9], first analyses regarding the intercell interference modeling for cellular MC-CDMA environments are given. A Gaussian approximation was proposed for the intercell interference modeling which was verified with more analytical investigations in [10, 11]. This simplified intercell interference assumption allows a large reduction of the simulation complexity for cellular MC-CDMA systems. In [12, 13] the main focus was on the overall performance of an MC-CDMA system in a cellular environment. It was shown that there exist large performance degradations in the cell border area. Even a sectorized cellular system could not reduce these degradations [14].

Theoretically, gains from using intercell interference avoidance schemes are large [15], but maximal gains would require fast and tight intercell coordination. For example, frequency partitioning in cellular networks on a slower time scale has for a long period received interest [16] as well as the use of power control [17], dynamic channel assignment, and

channel borrowing. Note that the packet-switched channel-aware scheduled transmissions which will take place in future systems complicate the use of many of the previously suggested schemes for intercell interference avoidance. For example, it is not, without additional side information, possible to conclude that the interference power in a set of subcarriers is likely to be higher/lower than average just because it is measured as high/low at present. Therefore, due to the orthogonal spread data symbols and the resulting redundancy in the transmission the spread spectrum technique MC-CDMA provides the possibility to iteratively remove the intercell interference at the receiver side without the need of high complex intercell interference management schemes from the network side.

This paper presents iterative intercell interference cancellation schemes for a cellular MC-CDMA downlink. An intercell interference cancellation (ICIC) scheme was already proposed in [18] by taking into account the hard decisions from the demodulator to reconstruct the signal and cancel the intercell interference. In this paper, we propose to use additional signal power information for the cancellation process which improves this *hard* ICIC process. More reliable information are the soft values from the outer channel decoder. Within a single MC-CDMA link the soft information is already used for iterative cancellation of the multiple access interference (MAI) [19]. It is possible to extend this principle to a cellular MC-CDMA downlink to cancel the intercell interference with a *soft* ICIC [20, 21]. Most cellular interference investigations on the link level are based on one interfering cell [8, 10, 12, 18, 20, 21] due to complexity constraints. This paper studies the influence of a cellular environment with a whole tier of interfering base stations around the desired base station. The extrinsic information of the decoding process is considered as a degree of reliability for the soft ICIC process.

In the following section, we first introduce the cellular MC-CDMA system and its cellular environment. Section 3 proposes different approaches of ICIC techniques. First, the hard decisions from the demodulator are used for the hard ICIC process. Further, an iterative ICIC technique based on soft values is presented in more detail which is named soft ICIC. The influence of intercell interference within a cellular environment is investigated in Section 4. Also in this section, the performances of the different ICIC schemes are compared by simulations.

2. CELLULAR MC-CDMA SYSTEM

2.1. MC-CDMA Transmitter

The MC-CDMA transmitter is shown in Figure 1. The system contains N_c subcarriers for N_u users. A channel-coder encodes the bit stream of each user. The encoded bits are interleaved by the outer interleaver Π_{out} and the interleaved code bits $\mathbf{c}^{(n)}$ of user n are passed to the symbol modulator. With respect to different modulation alphabets (e.g., PSK or QAM), the bits are modulated to complex-valued data symbols with the chosen cardinality. Before each modulated signal can be spread with a Walsh-Hadamard sequence of length $L \geq N_u$, a multiplexer (MUX) arranges the signals to $N_d \leq N_c/L$ parallel data symbols per user. For the case that $N_d = N_c/L$, the data stream is distributed over all available subcarriers. On the other hand, if $N_d < N_c/L$, other data streams are assigned to the remaining subcarriers, which are named user groups [7] and are independent from the aforementioned data stream. This guarantees equally loaded subcarriers. The kth symbol of all users, $\mathbf{d}_k = [d_k^{(1)}, \ldots, d_k^{(N_u)}]^T$, is multiplied with an $L \times N_u$ spreading matrix $\mathbf{C}_L$ resulting in

$$\mathbf{s}_k = \mathbf{C}_L \mathbf{d}_k, \quad \mathbf{s}_k \in \mathbb{C}, 1 \leq k \leq N_d. \tag{1}$$

In an MC-CDMA system, the system load is N_u/L and can be set to a value ranging from $1/L$ to 1. For maximizing the diversity gain, the block $\mathbf{s} = [\mathbf{s}_1, \ldots, \mathbf{s}_{N_d}]^T$ is frequency-interleaved by the inner random interleaver Π_{in} which represents one OFDM symbol. By taking into account a whole OFDM frame the interleaving can be done in two dimension, that is, time and frequency. $X_{l,i}^{(m)}$ denotes the value of the lth OFDM symbol in the ith subcarrier at base station (BS) m out of N_{BS}. Furthermore, N_s OFDM symbols describe one OFDM frame whereby each OFDM symbol has N_c subcarriers.

An OFDM modulation is performed on each block and contains operations as follows. First, an inverse FFT (IFFT) with $N_{FFT} \geq N_c$ points is done. Thus, the time domain signal is given by $x_{l,n}^{(m)} = \text{IFFT}\{X_{l,i}^{(m)}\}$, where $n = 1, \ldots, N_{FFT}$. Then, a guard interval (GI) in form of a cyclic prefix is inserted having N_{GI} samples. At the end of the transmitter a D/A conversion is carried out and $x^{(m)}(t)$ is obtained.

2.2. Cellular MC-CDMA receiver

Figure 2 depicts the receiver structure of the MC-CDMA system. The signal $x^{(m)}(t)$ is transmitted over a mobile radio channel and $y(t)$ is received. Then the inverse OFDM is performed including the removing of the GI and the FFT. We assume for the channel fading a quasi-static fading process, that is, the fading is constant for the duration of one OFDM frame. With this quasi-static channel assumption the well-known description of OFDM in the frequency domain is given.

After OFDM demodulation of the OFDM symbol, the received signal is

$$Y_{l,i} = \sum_{m=0}^{N_{BS}-1} X_{l,i}^{(m)} H_{l,i}^{(m)} + N_{l,i}, \tag{2}$$

where $H_{l,i}^{(m)}$ is the channel transfer function and $N_{l,i}$ is the additive white Gaussian noise (AWGN) with zero mean and variance N_0.

The inner deinterleaver Π_{in}^{-1} and a parallel-to-serial converter arranges the received signal to the kth spread symbol of the N_u users $\mathbf{r}_k = [r_{k,1}, \ldots, r_{k,L}]^T$. The entries of the despreader results from the linear minimum mean-squared error (MMSE) one tap equalizer $\mathbf{G}$ which restores the lost orthogonality between the spreading codes. Within a cellular

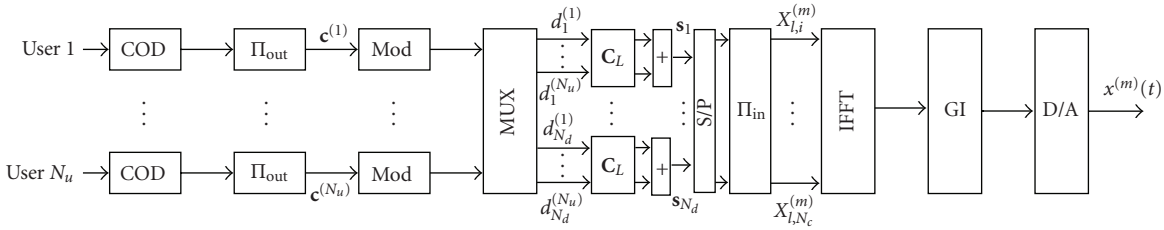

Figure 1: MC-CDMA transmitter of the mth base station.

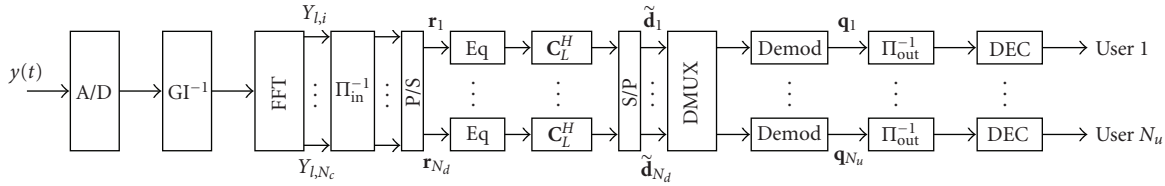

Figure 2: MC-CDMA receiver.

environment the MMSE has to be modified [11], resulting in the diagonal matrix entries

$$G_{i,i} = \frac{H_{l,i}^{(m)*}}{|H_{l,i}^{(m)}|^2 + \sigma^2 + \sum_{\substack{m'=0 \\ m' \neq m}}^{N_{\text{BS}}-1} E\left\{ |X_{l,i}^{(m')} H_{l,i}^{(m')}|^2 \right\}}, \quad (3)$$

where $\sigma^2 = (L/N_{\text{u}})(N_0/E_{\text{s}})$ is the actual variance of the noise and $\sum_{m'=0,m' \neq m}^{N_{\text{BS}}-1} E\{|X_{l,i}^{(m')} H_{l,i}^{(m')}|^2\}$ is the total power of the intercell interference. $(\cdot)^*$ denotes for complex conjugation. Therefore, the data symbols for the demodulator process result in

$$\mathbf{d}_k = \mathbf{C}_{\text{L}}^H \mathbf{G} \mathbf{r}_k = \left[\tilde{d}_k^{(1)}, \ldots, \tilde{d}_k^{(N_{\text{u}})} \right]^T. \quad (4)$$

All symbols of the desired user $\tilde{d}_k^{(1)}$ are combined to a serial data stream. Without loss of generality, we skip the symbol and user indices k and n for notational convenience in the following. The symbol demodulator demodulates the data symbols to real-valued soft-decisions q. In addition, it calculates the log-likelihood ratio (LLR) [22] for each code bit c by

$$L(c) = \log \frac{P(c = 0 \mid \tilde{d})}{P(c = 1 \mid \tilde{d})}. \quad (5)$$

The sign of $L(c)$ is the hard decision and the magnitude $|L(c)|$ is the reliability of the decision. The code bits are deinterleaved and decoded using the MAX-Log-MAP algorithm [23] which generates the LLR

$$L(c \mid \mathbf{q}) = \log \left(\frac{P(c = 0 \mid \mathbf{q})}{P(c = 1 \mid \mathbf{q})} \right). \quad (6)$$

In contrast to (5), the LLR value $L(c|\mathbf{q})$ is the estimate of all bits in the coded sequence $\mathbf{q}$ [19].

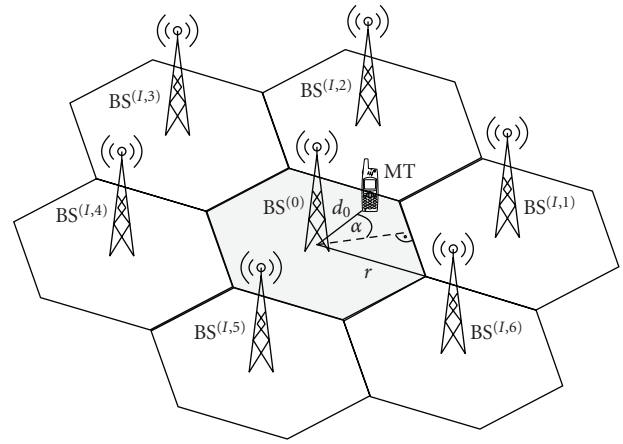

Figure 3: Cellular environment.

Another degree of reliability of the decoder output can be given by the expectation of $E\{c|\mathbf{q}\}$, the so-called soft bits [19, 24] which are defined by

$$\begin{aligned} \lambda(c|\mathbf{q}) &= (+1) \cdot P(c = 0 \mid \mathbf{q}) + (-1) \cdot P(c = 1 \mid \mathbf{q}) \\ &= \tanh\left(L(c \mid \mathbf{q})/2\right). \end{aligned} \quad (7)$$

These soft bits are in the range of $[-1, +1]$. The closer to the minimum or maximum, the more reliable the decoded bits are. There exists no reliable decision for $\lambda(c \mid \mathbf{q}) = 0$.

2.3. Cellular setup

We consider a synchronized cellular system in time and frequency. The mth BS has a distance d_m to the desired mobile terminal (MT) and the BSs are distributed in a hexagonal grid. We assume a normalized cell radius of one, and therefore, the distance is $d_0 = 1$ for $\alpha = 30°$. The cellular setting is illustrated in Figure 3.

The slowly varying signal power attenuation due to path loss is generally modeled as the product of the γth power of

distance d_m and a log-normal component representing shadowing losses [25]. γ represents the path loss factor and η_m is the Gaussian-distributed shadowing factor. Depending on the position of the MT the carrier-to-interference ratio (C/I) varies and is defined by

$$\frac{C}{I} = \frac{E\left\{ \left| X_{l,i}^{(0)} \cdot H_{l,i}^{(0)} \cdot d_0^{-\gamma} \cdot 10^{\eta_0/10\,\mathrm{dB}} \right|^2 \right\}}{\sum_{m=1}^{N_{\mathrm{BS}}-1} E\left\{ \left| X_{l,i}^{(m)} \cdot H_{l,i}^{(m)} \cdot d_m^{-\gamma} \cdot 10^{\eta_m/10\,\mathrm{dB}} \right|^2 \right\}}. \quad (8)$$

3. INTERCELL INTERFERENCE CANCELLATION

In this section we introduce different ICIC strategies. For most of interference cancellation schemes additional information is needed at the receiver. The receiver needs a detectable signaling from the involved BSs which can be given by an orthogonal signaling between the BSs. Further, a channel estimation process is needed for all impinging signals. On the other side, intercell interference cancellation schemes at the receiver avoid large configurations to reduce the intercell interference at the transmitter side, namely, the base stations and network. In the following, the concepts of hard and soft ICICs are introduced which try to remove the interfering signals from the desired signal. This can guarantee a more successful final decoding of the desired signal.

3.1. Hard ICIC

A first approach of ICIC is based on the use of the hard output of the demodulator at the receiver to reproduce the interfering or desired signals $\hat{Y}^{(m)}$. We name this process hard ICIC. In [18] three different combinations of the hard ICIC are proposed. Simplified block diagrams of the hard ICIC and its combinations are shown in Figures 4(a) and 4(b). Without loss of generality, we skip the subcarrier and time indices l and i for notational convenience in the following. We extend the already proposed hard ICIC concepts to more than one interfering cell. This is done by parallel processing of the reconstruction of the interfering signals ($m \neq 0$). All blocks are set up with their specific cell parameters. First, the *direct* hard ICIC (D-ICIC) with output

$$\hat{Y}_{\mathrm{D}} = Y - \sum_{m=1}^{N_{\mathrm{BS}}-1} \hat{Y}^{(m)} \quad (9)$$

can be seen as the basic concept block. Note that for the D-ICIC the processing of the interfering cells ($m \neq 0$) is used. The *indirect* hard ICIC (I-ICIC) tries to reconstruct the desired signal first and then the interfering signals. It should be mentioned that the estimated interfering signals will be subtracted in the final step from the received signal Y in contrast to Figure 4(b). Therefore, the I-ICIC calculates

$$\hat{Y}_{\mathrm{I}} = Y - \sum_{m=1}^{N_{\mathrm{BS}}-1} \hat{Y}_{\hat{Y}^{(0)}}^{(m)}, \quad (10)$$

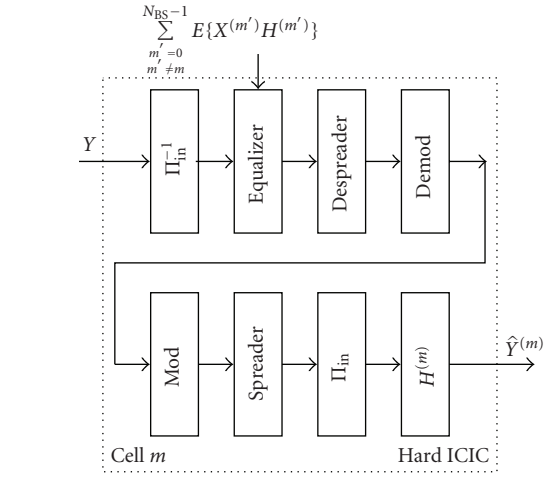

(a) Concept of the hard ICIC

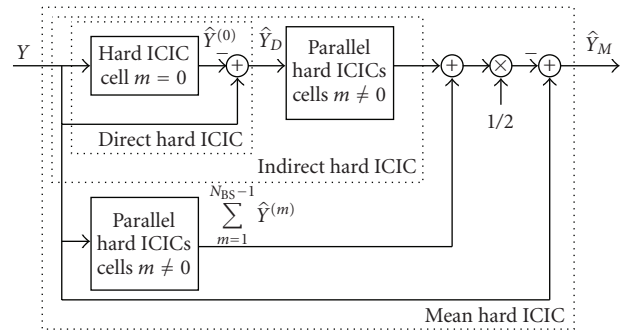

(b) Combinations of hard ICICs

Figure 4: Concept and combination of the hard ICIC.

where $\hat{Y}_{\hat{Y}^{(0)}}^{(m)}$ represents the estimates depending on the first estimate $\hat{Y}^{(0)} = Y - \hat{Y}^{(0)}$. The *mean* hard ICIC (M-ICIC) combines the D-ICIC and I-ICIC concepts by

$$\hat{Y}_{\mathrm{M}} = Y - 0.5\left(\sum_{m=1}^{N_{\mathrm{BS}}-1} \hat{Y}_{\hat{Y}^{(0)}}^{(m)} + \sum_{m=1}^{N_{\mathrm{BS}}-1} \hat{Y}^{(m)} \right). \quad (11)$$

All three concepts try to remove the intercell interference signals from the desired signal. In the final step, the output of the hard ICIC is taken to be demodulated and decoded.

Due to the use of orthogonal signaling between the cells, pilot signals can be used to achieve the received signal power, for example, if the communication system is sufficiently synchronized. Therefore, we propose to use this information for the equalization process (cf. (3)) in all ICIC concepts (cf. Figure 4(a)) which should influence and improve the overall performance of the hard ICICs.

3.2. Soft ICIC

A more sophisticated approach to cancel the intercell interference is based on the use of the more reliable soft values. In the following, we describe a soft ICIC technique for an arbitrary number of interfering cells. Figure 5 shows the block diagram of the proposed soft ICIC. The received signal

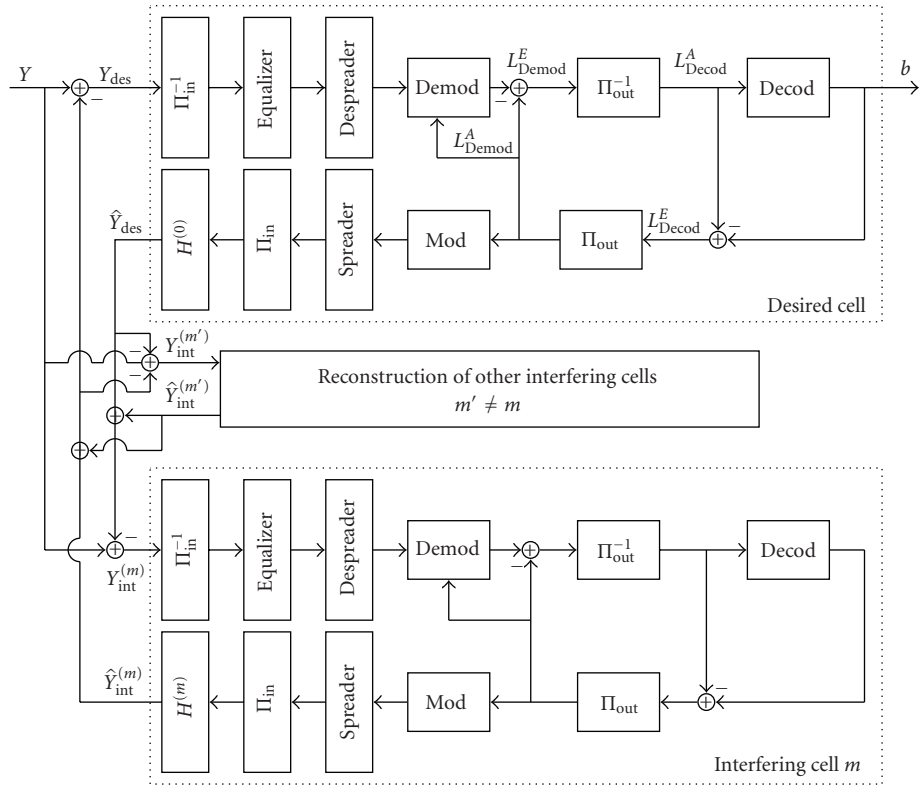

Figure 5: Concept of soft ICIC.

Y is processed as described in Section 2.2 in respect to its specific cell parameters m for the desired and intercell interference signals in parallel. In contrast to the hard ICIC process, the demodulator computes from the received symbols soft-demodulated extrinsic log-likelihood ratio values $L^{\mathrm{E}}_{\mathrm{Demod}}$. Unlike (5) without the use of a priori knowledge, the demodulator, and therefore, $L^{\mathrm{E}}_{\mathrm{Demod}}$ exploits the knowledge of a priori LLR-values $L^{\mathrm{A}}_{\mathrm{Demod}}$ with

$$L^{\mathrm{A}}_{\mathrm{Demod}} = \log \frac{P(c=0)}{P(c=1)} \tag{12}$$

coming from the decoder. $L^{\mathrm{E}}_{\mathrm{Demod}}$ is given by

$$L^{\mathrm{E}}_{\mathrm{Demod}}(c) = \log \frac{P(c=0 \mid \widetilde{d}, L^{\mathrm{A}}_{\mathrm{Demod}}(\mathbf{c}))}{P(c=1 \mid \widetilde{d}, L^{\mathrm{A}}_{\mathrm{Demod}}(\mathbf{c}))} - L^{\mathrm{A}}_{\mathrm{Demod}}(c). \tag{13}$$

In the initial iteration, the LLR-values $L^{\mathrm{A}}_{\mathrm{Demod}}$ for the demodulator are set to zero. After deinterleaving, the extrinsic LLR-values $L^{\mathrm{E}}_{\mathrm{Demod}}$ become the a priori LLR-values $L^{\mathrm{A}}_{\mathrm{Decod}}$ of the channel decoder. The channel decoder computes for all code bits the a posteriori LLR-values $L(c \mid \mathbf{q})$ using the MAX-Log-MAP algorithm (cf. (6)) and the extrinsic information $L^{\mathrm{E}}_{\mathrm{Decod}}$ is given by

$$L^{\mathrm{E}}_{\mathrm{Decod}} = L(c \mid \mathbf{q}) - L^{\mathrm{A}}_{\mathrm{Decod}}. \tag{14}$$

The extrinsic LLR-values $L^{\mathrm{E}}_{\mathrm{Decod}}$ are then interleaved to become the a priori LLR-values $L^{\mathrm{A}}_{\mathrm{Demod}}$ used in the next iteration in the demodulator. The signals of the desired cell $\widehat{Y}_{\mathrm{des}}$ and the interfering cells $\widehat{Y}^{(m)}_{\mathrm{int}}$ are reconstructed and for the next iteration step the inputs of the processing blocks are

$$\begin{aligned} Y_{\mathrm{des}} &= Y - \sum_{m=1}^{N_{\mathrm{BS}}-1} \widehat{Y}^{(m)}_{\mathrm{int}}, \\ Y^{(m)}_{\mathrm{int}} &= Y - \left(\widehat{Y}_{\mathrm{des}} + \sum_{\substack{m'=1 \\ m' \neq m}}^{N_{\mathrm{BS}}-1} \widehat{Y}^{(m')}_{\mathrm{int}} \right). \end{aligned} \tag{15}$$

The iterative cancellation process requires high computational complexity at the receiver and additionally introduces a delay to the signal processing. Each canceled interfering signal needs the same processing as the desired signal. Furthermore, this complexity is multiplied by the number of processed iterations.

In contrast to the hard ICIC concepts, the soft ICIC is not limited to one processing iteration. With this iterative approach, the intercell interference can be stepwise removed from the received signal.

4. SIMULATION RESULTS

The transmission system is based on a carrier frequency of 5 GHz, a bandwidth of 101.25 MHz, and an FFT length of $N_{\mathrm{FFT}} = 1024$. The number of used subcarriers is $N_{\mathrm{c}} = 768$ and the guard interval length is set to $N_{\mathrm{GI}} = 226$. Therefore, the sample duration is $T_{\mathrm{samp}} = 7.4$ nanoseconds. The spreading length L is set to 8. QPSK is used with set partitioning mapping throughout all simulations. The system runs either

Table 1: Parameters of the transmission system.

Carrier frequency	5 GHz
Bandwidth	101.25 MHz
No. of subcarriers	768
FFT length	1024
Guard interval length	226
Sample duration	7.4 ns
Frame length	16
Spreading length	8
Modulation	QPSK
Channel coding	CC $(561, 753)_8$
Channel coding rate	1/2

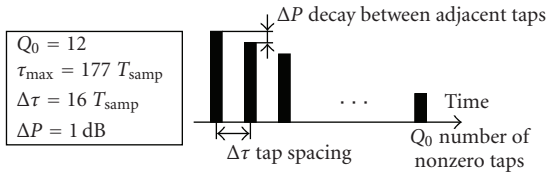

Figure 6: Parameters of the used power delay profile of the channel model.

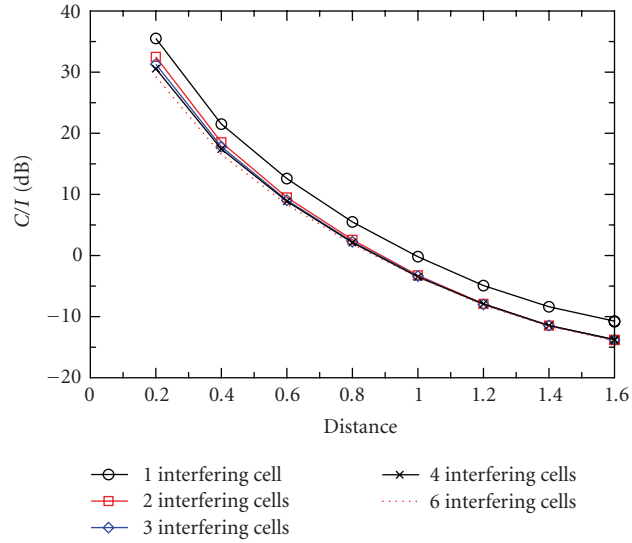

Figure 7: Influence of varying number of interfering cells on the C/I ratios at different MT positions.

in a half-loaded case or in a single-user mode. The interfering BSs have the identical parameters as the desired BS which also includes the number of active users. For the simulations, different signal-to-noise ratios (SNRs) are chosen and perfect channel knowledge of all cells is assumed. Furthermore, a $(561, 753)_8$ convolutional code with rate $R = 1/2$ was selected as channel code. A 2-dimensional random frequency interleaving is carried out. We assume i.i.d. channels with equal stochastic properties from each BS to the MT. The used channel model is a tapped delay-line model with equidistant 12 taps with a 1 dB decrease per tap and a maximum channel delay of $\tau_{max} = 1.31$ microseconds. The path loss factor is set to $\gamma = 4.0$ and the standard deviation of the Gaussian-distributed shadowing factor η_m is set to 8 dB for each cell. Table 1 summarizes the used simulation parameters and Figure 6 illustrates the power delay profile. In the following, we separate the simulation results in three blocks. First, we discuss the influence of the intercell interference; then, the simulation results of the different hard ICIC concepts are investigated; finally, the simulation results of the soft ICIC and its extrinsic information as reliability information are described.

4.1. Influence of intercell interference

Since the complexity of cancellation techniques depends directly on the number of paths or signals to be canceled, we investigate the influence of the neighboring signals to the overall interfering signal. Figure 7 shows the received C/I ratio at the mobile terminal for different locations within the cellular setup for a varying number of interfering cells. We assume that the MT moves along a straight line between the cell center and the outer part of the desired cell centered between two interfering BSs ($\alpha = 30°$). At the position $d_0 = 1.0$, the MT receives the same signal power from the three closest BSs. For these simulations, the order of interfering BSs are chosen by their decreasing distance to the MT. The closest interfering BS is the first and an SNR of 10 dB is given within all cells. Since the spreading combines the signals and all available subcarriers are allocated, there is no difference in the C/I ratio by varying the system load [26].

The simulation results for one interfering BS show at $d_0 = 1.0$ the expected C/I ratio of about 0 dB because both signals are received with the same power at this location. By increasing the number of interfering BSs a degradation of the C/I ratio over all MT positions is given. In the outer regions of the desired cell ($d_0 \geq 0.8$) there is no influence on the C/I ratio for more than two interfering BSs. In the inner part of the desired cell a small influence of the number of interfering cells is visible because the MT is nearly equidistant to all surrounding BSs. These results show that the main contribution of the intercell interference in a cellular MC-CDMA system is generated by the two closest interfering BSs. Therefore, it is appropriate and sufficient to take into account only the two strongest interfering signals for ICIC techniques.

4.2. Impact of hard ICIC

In the following, we verify the results in [18] by using the proposed hard ICIC concepts as described in Section 3.1. These hard ICIC techniques do not take into account the possible available signal powers for the equalization process. Figure 8 presents the bit-error rate (BER) performance versus the C/I ratio. The simulations are carried out with an SNR of 10 dB and within a two-cell environment where each cell is half loaded. Therefore, the low C/I values represent the outer part of the desired cell, $C/I = 0$ dB is the cell border, and positive C/I values are given in the inner cell area.

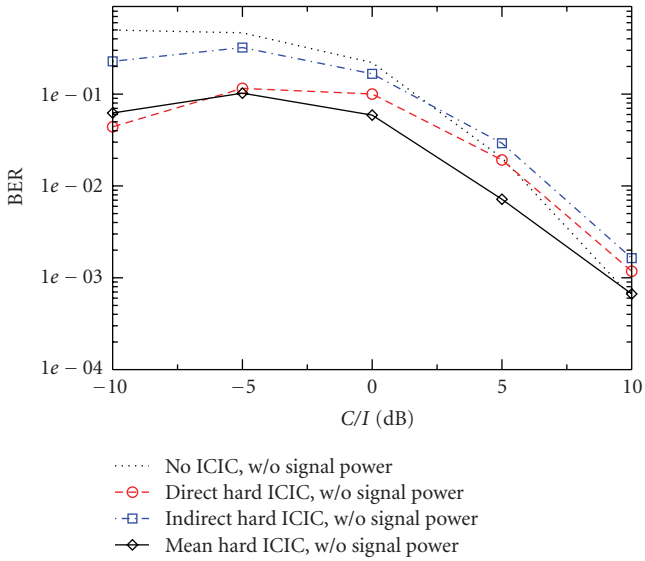

Figure 8: Performance of half-loaded system with different hard ICIC concepts in the cell border area with an SNR of 10 dB, without signal power knowledge.

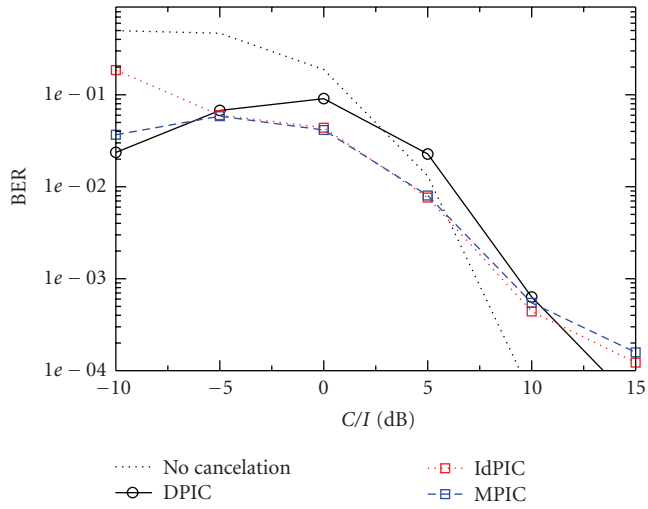

Figure 9: Performance of half-loaded system with different hard ICIC concepts in the cell border area with an SNR of 10 dB, with signal power knowledge.

All three hard ICIC concepts can increase the BER performance for low C/I values and at the cell border compared to the non-ICIC performance. The combination of D-ICIC and I-ICIC, namely, M-ICIC, can benefit from their performance behavior and provides the best performance. Only for $C/I \leq -5$ dB, M-ICIC performs worse than D-ICIC because the first component in the I-ICIC generates wrong estimates of the recovered signal. This is caused by the weak desired signal and the hard decided output. Since the decoding and re-encoding process is not used in the hard ICIC concept, the performances of the D-ICIC and I-ICIC suffer from wrong recovered signals in the reconstruction process for high C/I values. This should be avoided by the soft ICIC concept.

Figure 9 shows the performance gains of the different combinations for hard ICIC with the proposed knowledge of the received signal powers. Since the D-ICIC tries to remove only the interfering signal, it cannot profit from both signal powers and does not outperform the I-ICIC in contrast to Figure 8 and [18]. Only for high intercell interference scenarios the D-ICIC reconstructs and removes the interfering signal better than I-ICIC. There is no performances difference between the I-ICIC and M-ICIC for $C/I \geq -5$ dB. Only for larger intercell interference the M-ICIC benefits from the parallel D-ICIC for interfering cell $m = 1$ (cf. Figure 4(b)). But the inner I-ICIC still causes errors and the pure D-ICIC outperforms the M-ICIC.

By comparing Figures 8 and 9, we see a performance difference of the reference curves without an applied hard ICIC concept due to the knowledge of the interfering signal power. There is also a large performance gain for the hard ICIC concepts with the additional information of this power. In terms of the C/I ratio, the M-ICIC or I-ICIC can gain at the cell border about 2.5 dB with the additional power information compared to the M-ICIC without power knowledge.

4.3. Impact of soft ICIC

The influence to the performance within a cellular MC-CDMA system by applying a soft ICIC concept is shown in the following. It is possible to use the extrinsic information (cf. (14)) as a degree of reliability for the iterative process of the signal reconstruction. For the soft ICIC the mean of the absolute extrinsic information $L^{\mathrm{E}}_{\mathrm{Decod}}$ over all desired bits within one OFDM frame is taken to calculate a reliability information of the decoded signal in the jth iteration following the definition of soft bits (cf. (7)) by

$$\lambda_j = \tanh\left(\frac{1}{N}\sum_{n=0}^{N} |L^{\mathrm{E}}_{\mathrm{Decod}}|/2\right), \tag{16}$$

where N represents the total number of desired bits. Since the absolute value of $L^{\mathrm{E}}_{\mathrm{Decod}}$ is taken, the range of λ_j is now from $[0, 1]$. The lower λ_j the lower is the reliability of a correct reconstruction of the signal and vice versa. The difference

$$\Delta\lambda_{j+1,j} = \lambda_{j+1} - \lambda_j \tag{17}$$

represents the reliability change between the iterations. The a posteriori knowledge $L(c \mid \mathbf{q})$ (cf. (6)) is not taken into account in this paper which would give a measure of the resulting BER in the final decoding step [27].

A whole tier of cells, that is, 6 interfering cells, around the desired cell are assumed for the following investigations. The reliability information λ_j of the desired signal is simulated for positions of the mobile terminal in the range of $d_0 = [0.4, 1.4]$ around the desired BS. The SNR is set to 5 dB and the system is half loaded. Figure 10(a) shows λ_1 depending on the position for the first iteration of the soft ICIC in a three-dimensional illustration. It can be seen that in the inner part of the cell, ($d_0 \leq 0.6$) λ_1 is mostly 1.0. Therefore, the desired signal should be detected appropriately in this region. For the outer parts ($d_0 > 0.6$) there is a large degradation of the reliability for the decoding process. Differences

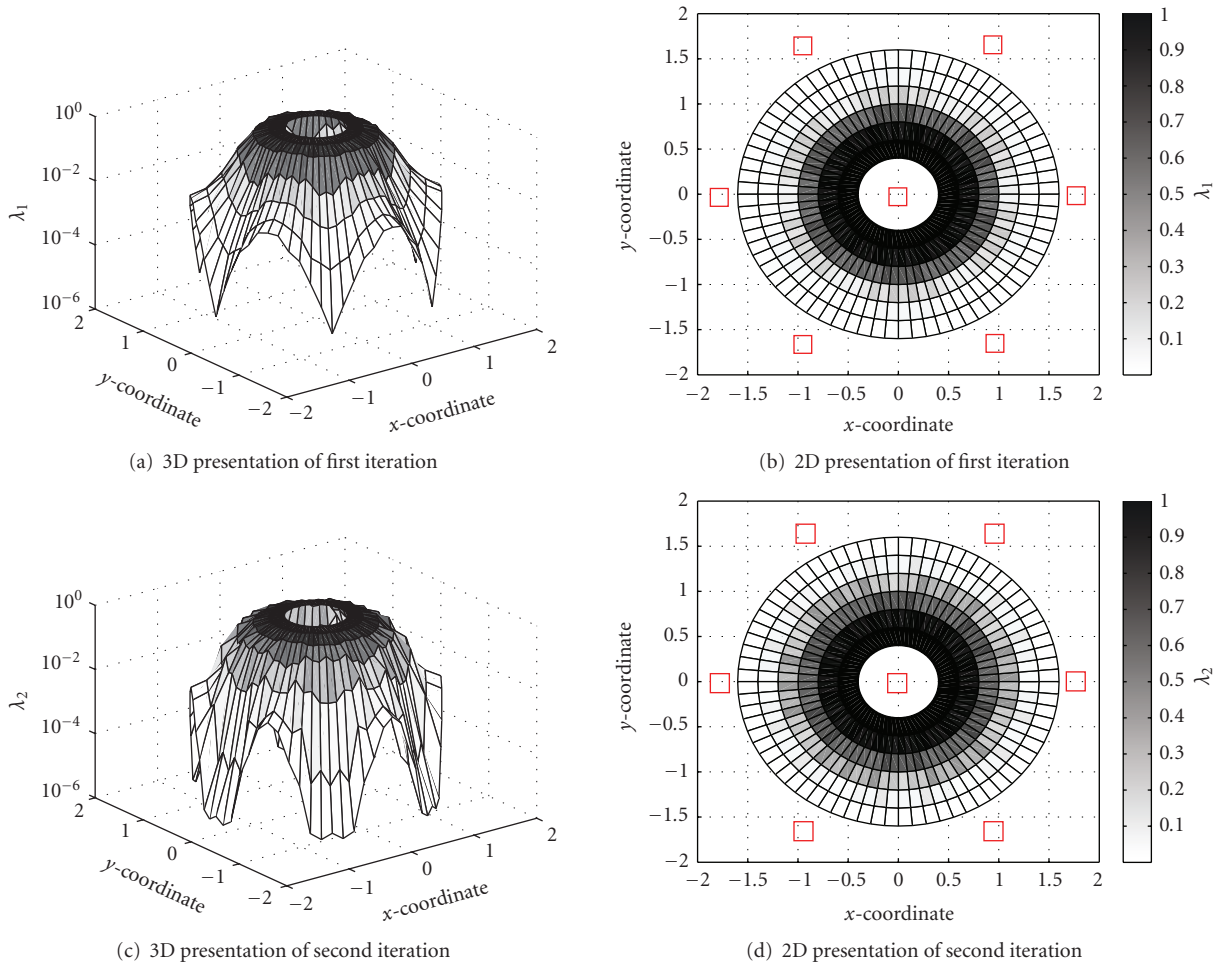

(a) 3D presentation of first iteration

(b) 2D presentation of first iteration

(c) 3D presentation of second iteration

(d) 2D presentation of second iteration

FIGURE 10: Resulting values of λ_j for the desired signal within the coverage of the desired base station depending on the position of the mobile terminal (base stations have rectangular markers) in two- and three-dimensional representations.

between the mobile terminal position are also visible, for example, the mobile terminal experiences one strong interfering BS ($(x, y) = (-1.4, 0)$) or the mobile terminal is located between two weaker interfering BSs ($(x, y) = (-1.2, -0.7)$). The distribution of λ_2 for the second iteration is shown in Figure 10(c). Already the second iteration can increase λ_2 over the whole area for this scenario compared to λ_1. Even in the cell border area, ($d_0 = [0.8, 1.2]$) λ_2 achieves values close to one. Therefore, this second iteration broadens the area for successful detection of the desired signal. Another representation of λ_j within the cellular environment is given in Figures 10(b) and10(d) for one and two iterations, respectively. The positions of the involved BSs are given by the rectangular marks. These plots show more precisely that in the first iteration the more reliable λ_1 values are limited to $d_0 < 1.0$. For the second iteration reliable, λ_2 values stretch already to $d_0 \leq 1.2$.

Due to the large simulation complexity of the whole cellular environment and its reproduction, we also provide the difference $\Delta\lambda_{2,1}$ in the three dimensional plot of Figure 11. It is clearly visible that the rim area gains in reliability for the decoding process for the second iteration. There are corridors without an increase of λ_2 due to the constellation of the cellular environment. Since the signal strength of the two closest interfering cells in these corridors (e.g., $\alpha = 30^\circ$) do not differ significantly, the soft ICIC process cannot improve the already good λ_1 values in the second iteration. If only one BS is the major interferer (e.g., $\alpha = 0^\circ$) and the signal strength between the desired and main interferer differs, the soft ICIC can detect both signals in the second iteration more precisely.

The distribution of λ_j depends directly on the chosen scenario. Figure 12 presents different SNR scenarios within a one-tier cellular environment. We investigate λ_j for the desired and the two closest interfering signals where the mobile terminal is located close to the cell border with almost the same distance to all these three BSs, that is, $d_0 = 0.9, \alpha = 30^\circ$, or $(x, y) = (0.78, 0.45)$. Due to the previous results in Section 4.1, the two closest interfering cells are taken into account for the soft ICIC process. Furthermore, we assume a single-user case within all cells. For low SNR values (SNR $\leq$ 0 dB), low and constant values of λ_j are given over all iterations. If the SNR is larger than 2 dB, λ_j increases for higher number of iterations. In the case of SNR = 8 dB, there

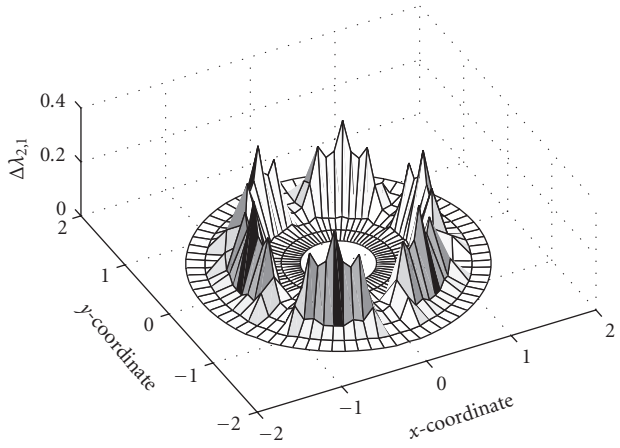

FIGURE 11: Difference $\Delta\lambda_{2,1} = \lambda_2 - \lambda_1$ of the reliability information between the first and second iterations of the soft ICIC process.

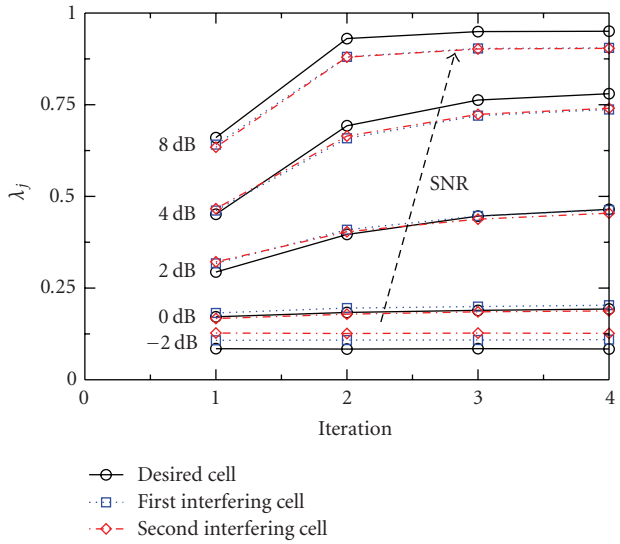

FIGURE 12: Reliability of decoding process of recovering the signals of different cells close to the cell border for several iterations at varying SNR scenarios.

exists a large step between the first and second iteration but the following iterations do not increase λ_j for $j > 2$ anymore. Due to the small power differences of the three received signal ($d_0 = 0.9$), the reliability information λ_j varies for the detected signals. It is obvious that a higher SNR provides better detection possibilities than low SNR scenarios for the desired signal.

The same simulation setup is chosen for Figure 13 except that this single-user scenario is directly located at the cell border ($d_0 = 1.0, \alpha = 30°$). The performance regarding the BER versus SNR is given. As an upper bound of the system, the performance with no ICIC is illustrated. The lower bound is represented by the single-user performance without any intercell interference. Already the first iteration increases the performance for SNR > 2 dB. The second iteration can increase the performance significantly which con-

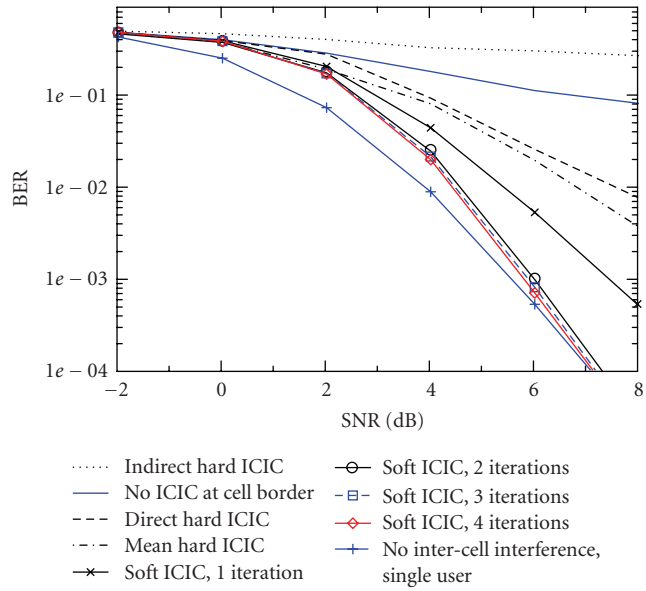

FIGURE 13: Performance of the soft ICIC for the single-user case at the cell border for different SNR values.

firms the characteristics of the λ_j values in Figure 12. Even the single-user bound can be almost reached within 2 iterations for higher SNRs. With 4 iterations it is possible to reach the single-user bound, and therefore, the intercell interference is removed.

For comparison we included the performance curves of the hard ICIC concepts in Figure 13. Since no decoding is taken into account in this cancellation technique, the performance does not reach the first iteration performance of the soft ICIC. Still the M-ICIC and D-ICIC can improve the performance significantly compared to no applied ICIC. In contrast to a two-cell scenario (cf. Figure 9), the I-ICIC cannot handle the intercell interference of several interfering cells appropriately, and therefore, there exists a large performance loss.

The performance in the cell border area for the soft ICIC is presented in Figure 14. The SNR is set to 10 dB and the system is half loaded in all seven cells. The desired and the two closest interfering cells are chosen to be processed in the soft ICIC. The mobile terminal moves along a straight line from $d_0 = 0.6$ to $d_0 = 1.6$ with $\alpha = 30°$. The performance without any applied ICIC technique is represented by the dotted line. For this scenario the first iteration cannot cancel out the intercell interference. Therefore, the hard ICIC concepts also fail for this scenario, represented by the M-ICIC performance. The second iteration of soft ICIC can achieve a small performance improvement. The so-called turbo cliff is reached with the third iteration and large performance gains can be achieved. A fourth iteration yields no appreciable improvement. All performance curves merge to the non-ICIC curve if they reach the intercell interference free case ($d_0 < 0.8$). Directly at the cell border ($d_0 = 1.0$) all processed signals are received with the same power, and therefore, the signals are at most difficult to separate and the soft ICIC performance is worst at this point. Due to the different received

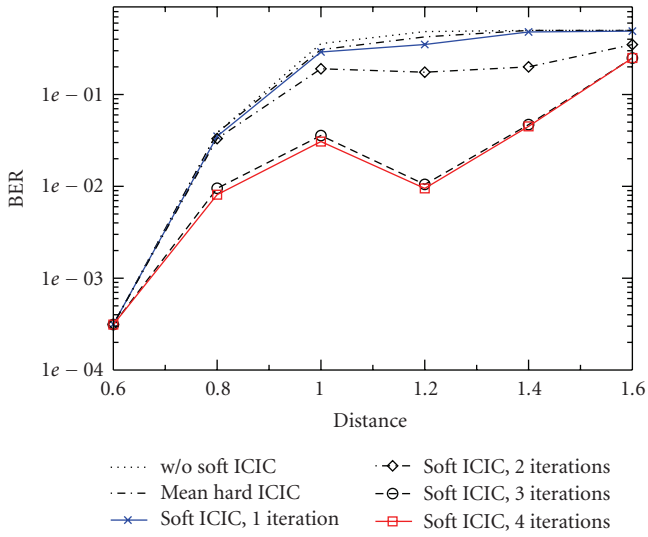

Figure 14: Performance of a half-loaded system with soft ICIC in the cell border area with an SNR of 10 dB.

signal powers, the soft ICIC can maximize the performance at $d_0 = 1.2$. This performance is similar to the almost inter-cell interference free case at $d_0 = 0.8$. For larger distances to the desired BS ($d_0 > 1.2$), the performance degrades because the desired signal becomes weak and the final decoding step for the desired signal can fail.

We can conclude from these investigations that the less complex hard ICIC concepts can be beneficial in scenarios where the impinging signals can be well distinguished. This correlates directly to the behavior of the decoding capability of the first iteration in the soft ICIC. The more complex soft ICIC technique is more robust to different scenarios and can improve the performance significantly by using several iterations. Due to the larger complexity of the soft ICIC, this technique can be applied at receivers with the available processing capabilities.

5. CONCLUSIONS

In this paper, we have described and investigated several approaches of intercell interference cancellation (ICIC) schemes in a cellular MC-CDMA downlink environment. The hard ICIC takes into account the hard decided output of the demodulator and with the proposed use of the signal power information the overall performance benefits. A more sophisticated approach is based on the use of the soft outputs of the decoder to reconstruct the signals for cancellation. Both schemes can improve significantly the performance in the severe cell border area. Performance results show that the soft ICIC approaches the single-user bounds without inter-cell interference, and therefore, the interference of the cellular environment can be almost eliminated. The extrinsic information of the decoding process can give a reliability information about the successful decoding process, and therefore, the behavior of the soft ICIC for different scenarios can be described and analyzed. The profit of the soft ICIC depends directly on the given scenarios and the used number of iterations.

REFERENCES

[1] IST-4-027756 WINNER Project, https://www.ist-winner.org/.
[2] J. A. C. Bingham, "Multicarrier modulation for data transmission: an idea whose time has come," *IEEE Communications Magazine*, vol. 28, no. 5, pp. 5–14, 1990.
[3] Z. Wang and G. B. Giannakis, "Wireless multicarrier communications: where Fourier meets Shannon," *IEEE Signal Processing Magazine*, vol. 17, no. 3, pp. 29–48, 2000.
[4] K. Fazel and L. Papke, "On the performance of convolutionally-coded CDMA/OFDM for mobile communications systems," in *Proceedings of the IEEE International Symposium on Personal, Indoor and Mobile Radio Communications (PIMRC '93)*, pp. 468–472, Yokohama, Japan, September 1993.
[5] N. Yee, J.-P. Linnartz, and G. Fettweis, "Multi-carrier CDMA for indoor wireless radio networks," in *Proceedings of the IEEE International Symposium on Personal, Indoor and Mobile Radio Communications (PIMRC '93)*, pp. 109–113, Yokohama, Japan, September 1993.
[6] S. Weinstein and P. Ebert, "Data transmission by frequency-division multiplexing using the discrete Fourier transform," *IEEE Transactions on Communications*, vol. 19, no. 5, part 1, pp. 628–634, 1971.
[7] K. Fazel and S. Kaiser, *Multi-Carrier and Spread Spectrum Systems*, John Wiley & Sons, New York, NY, USA, 2003.
[8] G. Auer, S. Sand, A. Dammann, and S. Kaiser, "Analysis of cellular interference for MC-CDMA and its impact on channel estimation," *European Transactions on Telecommunications*, vol. 15, no. 3, pp. 173–184, 2004.
[9] S. Plass, S. Sand, and G. Auer, "Modeling and analysis of a cellular MC-CDMA downlink system," in *Proceedings of the 15th IEEE International Symposium on Personal, Indoor and Mobile Radio Communications (PIMRC '04)*, vol. 1, pp. 160–164, Barcelona, Spain, September 2004.
[10] X. G. Doukopoulos and R. Legouable, "Impact of the inter-cell interference in DL MC-CDMA systems," in *Proceedings of the 5th International Workshop on Multi-Carrier Spread-Spectrum (MC-SS '05)*, pp. 101–109, Oberpfaffenhofen, Germany, September 2005.
[11] S. Plass, X. G. Doukopoulos, and R. Legouable, "On MC-CDMA link-level inter-cell interference," in *Proceedings of the 65th IEEE Vehicular Technology Conference (VTC '07)*, pp. 2656–2660, Dublin, Ireland, April 2007.
[12] F. Bauer, E. Hemming, W. Wilhelm, and M. Darianian, "Inter-cell interference investigation of MC-CDMA," in *Proceedings of the 61st IEEE Vehicular Technology Conference (VTC '05)*, vol. 5, pp. 3048–3052, Stockholm, Sweden, May-June 2005.
[13] S. Plass, "Hybrid partitioned cellular downlink structure for MC-CDMA and OFDMA," *Electronics Letters*, vol. 42, no. 4, pp. 226–228, 2006.
[14] S. Plass and A. Dammann, "On the error performance of sectorized cellular systems for MC-CDMA and OFDMA," in *Proceedings of the 16th IEEE International Symposium on Personal, Indoor and Mobile Radio Communications (PIMRC '05)*, vol. 1, pp. 257–261, Berlin, Germany, September 2005.
[15] M. K. Karakayali, G. J. Foschini, and R. A. Valenzuela, "Network coordination for spectrally efficient communications in cellular systems," *IEEE Wireless Communications*, vol. 13, no. 4, pp. 56–61, 2006.

[16] I. Katzela and M. Naghshineh, "Channel assignment schemes for cellular mobile telecommunication systems: a comprehensive survey," *IEEE Personal Communications*, vol. 3, no. 3, pp. 10–31, 1996.

[17] N. Feng, S.-C. Mau, and N. B. Mandayam, "Pricing and power control for joint network-centric and user-centric radio resource management," *IEEE Transactions on Communications*, vol. 52, no. 9, pp. 1547–1557, 2004.

[18] X. G. Doukopoulos and R. Legouable, "Intercell interference cancellation for MC-CDMA systems," in *Proceedings of the 65th IEEE Vehicular Technology Conference (VTC '07)*, pp. 1612–1616, Dublin, Ireland, April 2007.

[19] S. Kaiser and J. Hagenauer, "Multi-carrier CDMA with iterative decoding and soft-interference cancellation," in *Proceedings of the IEEE Global Telecommunications Conference (GLOBECOM '97)*, vol. 1, pp. 6–10, Phoenix, Ariz, USA, November 1997.

[20] M. Chacun, M. Hélard, and R. Legouable, "Iterative intercell interference cancellation for DL MC-CDMA systems," in *Proceedings of the 6th International Workshop on Multi-Carrier Spread Spectrum*, S. Plass, A. Dammann, S. Kaiser, and K. Fazel, Eds., vol. 1, pp. 277–286, Springer, Herrsching, Germany, May 2007.

[21] S. Plass, "Investigations on soft inter-cell interference cancellation in OFDM-CDM systems," in *Proceedings of the 12th International OFDM Workshop (InOWo '07)*, Hamburg, Germany, August 2007.

[22] J. Hagenauer, E. Offer, and L. Papke, "Iterative decoding of binary block and convolutional codes," *IEEE Transactions on Information Theory*, vol. 42, no. 2, pp. 429–445, 1996.

[23] P. Robertson, E. Villebrun, and P. Hoeher, "A comparison of optimal and sub-optimal MAP decoding algorithms operating in the log domain," in *Proceedings of the IEEE International Conference on Communications (ICC '95)*, vol. 2, pp. 1009–1013, Seattle, Wash, USA, June 1995.

[24] P. A. Hoeher, P. Robertson, E. Offer, and T. Woerz, "The soft-output principle reminiscences and new developments," *European Transactions on Telecommunications*, 2007.

[25] G. D. Ott and A. Plitkins, "Urban path-loss characteristics at 820 MHz," *IEEE Transactions on Vehicular Technology*, vol. 27, no. 4, pp. 189–197, 1978.

[26] S. Plass, A. Dammann, and S. Kaiser, "Error performance for MC-CDMA and OFDMA in a downlink multi-cell scenario," in *Proceedings of the 14th IST Mobile & Wireless Communications Summit (IST Summit '05)*, Dresden, Germany, June 2005.

[27] S. ten Brink, "Convergence behavior of iteratively decoded parallel concatenated codes," *IEEE Transactions on Communications*, vol. 49, no. 10, pp. 1727–1737, 2001.